

Characterization of Elastic, Dielectric and Piezoelectric Properties of Piezoelectric Materials

Wenwu Cao
Materials Research Laboratory
The Pennsylvania State University, University Park, PA 16802

ABSTRACT

Both the resonance and ultrasonic techniques are standard methods for characterizing the physical properties of piezoelectric materials. However, we found that each technique can only offer a few reliable measurements while the rest often have errors or impossible to implement because of the sample requirements. This paper show that one can use the combination of both techniques to achieve much better accuracy and be able to get the complete set of elastic, dielectric and piezoelectric coefficients using fewer samples. Using an ultrasonic spectroscopy we have also measure the dispersion of the ultrasonic velocity and the attenuation up to 65 MHz. $\text{Pb}(\text{Zr,Ti})\text{O}_3$ [PZT] ceramics were used as examples for both studies.

Keyword: Ultrasonic measurement, resonance, piezoelectric ceramic, PZT, elastic constant, piezoelectric constant, dielectric constant.

1. INTRODUCTION

The qualities of piezoelectric materials are described by basic physical parameters, such as the piezoelectric, dielectric, and elastic constants, and electromechanical coupling factors. A number of methods, including static, quasi-static, resonance and pulse-echo ultrasonic techniques,¹⁻³ have been used to measure these material constants. Depending on the symmetry of the piezoelectric system, the number of independent constants will be quite different. This symmetry refers to the macroscopic symmetry, not the microscopic symmetry unless for single domain single crystals. In the case of piezoelectric ceramics, the symmetry is homogenous before poling and ∞m after poling irrespective of the microscopic symmetry, the number of independent property tensors is the same as those of point group $6mm$.⁴

The resonance method for the measurement of piezoelectric materials are described in IRE and IEEE standards.^{5,6} In the resonance method, some specific resonance modes may be excited by applying a variable frequency A.C. field to piezoelectric samples of specific shape, aspect ratio and polarization orientation. The resonance frequency f_r and anti-resonance frequency f_a can be recorded from the impedance frequency spectrum. All physical parameters except the dielectric the constants, can be calculated from these resonance and anti-resonance frequencies according to the dynamic equations for these piezoelectric vibrators. The resonance method can also be used to measure piezoelectric single crystals. However, if the symmetry is low, more samples are needed with different geometry and aspect ratio.⁷ Because only small size crystals are available for many new crystals and domain switching may also occur, it is difficult to meet the large aspect ratio requirement in single domain single crystal state. Therefore, the resonance method alone can not determine all the material constants.

The ultrasonic pulse-echo method is frequently used to determine the elastic constants of solid materials of different symmetries.⁸⁻¹¹ By sending shear and longitudinal waves into several plates of specified orientations, all material constants can be measured from the wave propagation velocities. The ultrasonic method is often more accurate than the resonance method because it is performed under non-

resonance conditions, hence no mode interference. However, the solutions of the Christoffel equations for piezoelectric materials of lower symmetry are usually coupled and are difficult to solve. Large errors may be introduced while extracting these constants from the coupled modes.

With these considerations, we have developed a combined technique that uses a length longitudinal bar to supplement the ultrasonic technique to measure the electromechanical coupling factor k_{33} and the elastic compliance s_{33}^E . This combined method can provide a complete set of elastic, dielectric, and piezoelectric coefficients with minimum error. As an example, the elastic, piezoelectric and dielectric constants of PZT piezoelectric ceramic have been determined.

2. GENERAL PRINCIPLE OF ULTRASONIC MEASUREMENT

The propagation velocities of ultrasonic plane waves measured for various propagation and polarization direction produce a set of effective elastic stiffness constants through the product of the density of material and the velocity square. These effective elastic stiffness constants are related to the elastic, piezoelectric and dielectric constants by the general equations of motion for elastic plane wave propagation in a piezoelectric solid.

The equation of motion for particle displacements u_k associated with plane traveling waves can be written as⁸

$$(\Gamma_{ik} - \delta_{ik}\rho V^2)u_k = 0, \quad (1)$$

where

$$\Gamma_{ik} = \bar{c}_{ijkl}n_j n_l \quad (2)$$

is the Christoffel stiffness tensor for an arbitrary propagation direction \mathbf{n} , and

$$\bar{c}_{ijkl} = c_{ijkl}^E + \frac{e_{pij}e_{qkl}n_p n_q}{\epsilon_{rs}^s n_r n_s} \quad (3)$$

is the effective elastic stiffness tensor of a piezoelectric crystal. The symbol ρ and V denote density of the material and the phase velocity of the elastic plane wave, while c_{ijkl}^E , e_{pij} , ϵ_{rs}^s represent the components of the constant field elastic stiffness tensor, piezoelectric stress tensor, and dielectric tensor under constant strain, respectively. For nontrivial solutions, the determinant of the coefficients of u_k must vanish, or

$$|\Gamma_{ik} - \delta_{ik}\rho V^2| = 0. \quad (4)$$

Eq.(4) yields three positive real eigenvalues ρV^2 ($j=1,2,3$) for each specified propagation direction \mathbf{n} .

As an example, we introduce the general procedure of using ultrasonic pulse-echo method to get a full set of independent physical parameters for a poled PZT-5H ceramic sample, which has a symmetry group ∞m . Assuming the sample is poled in the z-direction, the relationships between the velocities and the elastic constants are given in Table I together with the measured velocities. Four elastic stiffness constants c_{11}^E , c_{12}^E , c_{44}^E and c_{66}^E , one piezoelectric constants e_{15} , and one clamped dielectric constant ϵ_{11}^s may be calculated directly from the measurements of the phase velocities with pure modes along [100], [001] and [110] crystallographic directions, respectively, when ϵ_{11}^r is known.

Table I: Effective elastic constants $\Lambda_{ik} = \rho V^2$ for class and $6mm$ ($\mathbf{P} = [0,0,P]$), and measured ultrasonic phase velocities V and \bar{c} for a piezoelectric ceramic PZT-5H

Mode No.	Sample thickness (mm)	Propagation direction	Polarization displacement	Wave type	$\bar{c} = \rho V^2$	Phase velocity (m/sec)	Effective elastic stiffness constant ($\times 10^{10}$ N/m ²)
1	2.13	[100]	[100]	L	c_{11}^E	3922.7	11.3
2			[010]	S	c_{66}^E	1767.6	2.30
3			[001]	S	$c_{44}^D = c_{44}^E + e_{13}^2 / 4\epsilon_{33}^S$	2209.5	3.56
4	3.13	[001]	[100]	S	c_{44}^E	1651.7	2.01
5			[001]	L	$c_{33}^D = c_{33}^E + e_{33}^2 / \epsilon_{33}^S$	4293.6	13.6
6	2.56	[110]	[1 $\bar{1}$ 0]	S	$(c_{11}^E - c_{12}^E) / 2$	1762.1	2.29
7	2.91	[101]	[10 $\bar{1}$]	QS	c_{101}^{qs}	1929.7	2.74
8			[101]	QL	c_{101}^{ql}	4133.5	12.6
9	5.30	[111]	[111]	QL	c_{111}^{ql}	1981.3	12.3
10			[11 $\bar{2}$]	QS	c_{112}^{qs}	4094.2	2.89

where L: longitudinal; S: shear; QL: quasi-longitudinal; QS: quasi-shear, and the new quantities in the table are given by

$$c_{10\bar{1}}^{qs} = (c_{11}^E + c_{33}^E + 2c_{44}^E) / 4 + E_{31}^2 + E_{33}^2 - \left\{ (c_{11}^E - c_{33}^E) / 4 + E_{31}^2 - E_{33}^2 \right\} + \left[(c_{13}^E + c_{44}^E) / 2 + 2 \cdot E_{31} \cdot E_{33} \right]^{1/2}$$

$$c_{101}^{ql} = (c_{11}^E + c_{33}^E + 2c_{44}^E) / 4 + E_{31}^2 + E_{33}^2 + \left\{ (c_{11}^E - c_{33}^E) / 4 + E_{31}^2 - E_{33}^2 \right\} + \left[(c_{13}^E + c_{44}^E) / 2 + 2 \cdot E_{31} \cdot E_{33} \right]^{1/2}$$

$$c_{111}^{ql} = (c_{11} + c_{12} + c_{33} + 3c_{44} + 2c_{66}) / 6 + E_{31}^2 / 12 + E_{33}^2 / 6 + \left\{ (c_{11} + c_{12} - c_{33} - c_{44} + 2c_{66} + E_{31}^2 / 2 - E_{33}^2) \right\} + 8 \left[(c_{13} + c_{44}) + E_{31} \cdot E_{33} / 2 \right]^{1/2} / 6$$

$$c_{11\bar{2}}^{qs} = (c_{11}^E + c_{12}^E + c_{33}^E + 3c_{44}^E + 2c_{66}^E) / 6 + E_{31}^2 / 12 + E_{33}^2 / 6 - \left\{ (c_{11}^E + c_{12}^E - c_{33}^E - c_{44}^E + 2c_{66}^E + E_{31}^2 / 2 - E_{33}^2) \right\} + 8 \left[(c_{13}^E + c_{44}^E) + E_{31} \cdot E_{33} / 2 \right]^{1/2} / 6$$

$$E_{31} = \frac{e_{15} + 2e_{31}}{4(\epsilon_1 + \epsilon_3)^{1/2}}; \quad E_{33} = \frac{e_{15} + 2e_{33}}{4(\epsilon_1 + \epsilon_3)^{1/2}}; \quad E_{31}' = \frac{e_{15} + 2e_{31}}{(2\epsilon_1 + \epsilon_3)^{1/2}}; \quad E_{33}' = \frac{e_{15} + e_{33}}{(2\epsilon_1 + \epsilon_3)^{1/2}}.$$

The remaining five constants $c_{13}^E, c_{33}^E, e_{13}, e_{33}$ and ϵ_{33}^S , in principle, may be evaluated from phase velocity measurements along propagation directions of [001], [101] and [111] and the measurement of ϵ_{33}^T . There are, however, numerical problems, particularly when the piezoelectric constants are small compared to the elastic properties. We found that the piezoelectric constants, d_{33} and d_{31} , will be easier to be determined from the measurements of electromechanical coupling factors and the resonance and anti-resonance frequencies of piezoelectric vibrators. In other words, more accurate results can be obtained by combining the two techniques.

3. MEASURED MATERIAL CONSTANTS FOR POLED PZT CERAMIC

We will use PZT ceramic as an example to show the effectiveness of the combined characterization method. The measured results using the combined method and a set of data obtained from conventional resonance technique are listed in Table II for comparison. Although c_{66}^E is not an independent constant in the measurement of the ceramic sample, it has been included for completeness since it represents one of the direct measured quantities. The dielectric constants, ϵ_{33}^T and ϵ_{11}^T , were calculated based on the parallel plate capacitance approximation. There are three complete sets of physical constants of PZT-5H are listed in Table II. The data in the column M-1 were derived from the independent constants, $c_{11}^E, c_{12}^E, c_{44}^E, c_{66}^E, e_{15}$, determined from ultrasonic measurements, and the constants $s_{11}^E, s_{33}^E, d_{31}, d_{33}$, were determined from resonance technique. The data in the column M-2 of Table II were derived from the independent constants, $c_{11}^E, c_{12}^E, c_{13}^E, c_{44}^E, c_{66}^E, e_{15}, e_{31}$, determined from ultrasonic measurements, and s_{33}^E and d_{33} , which were determined from a length longitudinal vibrator. The data in the column M-3 were derived from the standard resonance technique using four samples with different geometry. We can see that data in columns M-1 and M-2 are much closer to each other than to the data listed in column M-3. In addition, the combined method used one sample less than the resonance method and used only the clear modes, which reduced the uncertainties.

4. FREQUENCY DEPENDENCE OF VELOCITIES AND ATTENUATION IN PZT

The measured data given in Table II are for low frequencies. It was found that the velocity dispersion is not significant below for PZT ceramics, however, the attenuation, which corresponds to the imaginary part of the elastic constant, depends strongly on frequency. The dispersion information is very important for design high frequency transducers. In order to address this problem, we have built a special high frequency ultrasonic equipment which can measure the dispersion of velocity and attenuation up to 65 MHz. The diagram of the experimental set up is shown in Fig. 1. One pair of transducers with a center frequency of 50MHz and bandwidth of 80% were immersed in a water tank as the transmitter and receiver. A plate sample is fixed onto a computer controlled rotating table, which allows the ultrasonic wave to enter the sample surface at any desired angle. The output waveform was recorded by a digital oscilloscope (Tektronix TDS 460A) at a sampling rate of 10Gs/sec. The data were then transferred into a PC computer via a GPIB interface.

The experiments were conducted in two steps. First, a reference signal was collected without the sample in between the two transducers. This signal was then converted into frequency domain signals using the Fast Fourier Transform. Next, the sample was put in between the two transducers as shown in Fig.1 and the ultrasonic signal was again collected. This new signal and the reference signal can be used to calculate the ultrasonic velocity and the attenuation in the frequency range within the bandwidth of the transducer, detailed mathematical derivation can be found in Ref. [12].

Two PZT samples were made, which we name them PZT_z and PZT_x. The orientations of the two samples and the wave incidence planes are illustrated in Fig. 2. When measuring the longitudinal velocities, the ultrasonic wave enters the sample along the surface normal direction. When measuring the shear velocities on the other hand, the ultrasonic beam enters the sample at the critical angle of the longitudinal wave so that only the shear wave propagates inside the PZT. This mode conversion effect enables us to obtain the high frequency shear velocity value using a longitudinal transducer.¹²

By adjusting the ultrasonic beam incidence angle to the two PZT samples, we can determine the dispersion of velocities and attenuation in the following acoustic modes:

A). For the PZT_z sample:

1. Longitudinal wave propagating along the poling direction with the wave normal incident upon the plate. From the velocity dispersion of this wave, the frequency dependence of the elastic constant c_{33}^D can be determined.
2. Quasishear wave propagating in the x-z plane with the wave obliquely incident at the critical angle of the longitudinal wave. From its velocity dispersion one can determine an elastic constant combination c^* and its frequency dependence (see ref. 12 for the form of c^* and its derivation).

B). For the PZT \bar{x} sample:

1. Longitudinal wave propagating perpendicular to the poling direction. From its velocity dispersion one can determine the elastic constant c_{11}^E and its frequency dependence.
2. Shear wave with directions of propagation and polarization normal to the poling direction and the wave is incident at the critical angle of the longitudinal wave. From the velocity dispersion of this wave one can determine the elastic constant c_{66}^E and its frequency dependence.

The measurement results are shown in Figs. 3-6, for the phase velocities and attenuation in the two samples, respectively. It was observed that velocity dispersion exists for both the longitudinal and shear waves in the frequency range of the measurement and it is nearly linear, but the attenuation exhibits nonlinear frequency dependence. The attenuation of the shear wave is an order of magnitude higher than that of longitudinal wave.

If a medium in which an acoustic wave propagates can be considered as linear and causal system, its attenuation, which is associated with the imaginary part of the elastic modulus, and the velocity dispersion, which is associated with the real part of elastic modulus, are related by the Kramers-Kronig relations.¹² The approximation forms of the nearly local relationships can be expressed as:

$$v(\omega) = v(\omega_0) + \frac{2v^2(\omega_0)}{\pi} \int_{\omega_0}^{\infty} \frac{\alpha(\omega)}{\omega^2} d\omega \quad (5)$$

$$\alpha(\omega) = \frac{\pi\omega^2}{2v^2(\omega_0)} \frac{dv(\omega)}{d\omega} \quad (6)$$

where ω_0 is the starting frequency at which the velocity $v(\omega_0)$ and attenuation $\alpha(\omega_0)$ are known. In our experiment, $\omega_0 = 2\pi \cdot 20\text{MHz}$.

The ultrasonic spectroscopy technique is inherently based on the assumption of linearity. Thus, the velocity dispersion and attenuation obtained from the technique are expected to satisfy the above Kramers-Kronig relations. To verify the validity of these relations, the measured attenuation for the PZT-5H samples was fitted as a polynomial function of frequency, then the phase velocity dispersion was derived by the first Kramers-Kronig relation Eq.(5), then these calculated results were compared to measured results. As shown in Figs. 3 and 4 that the agreement is quite acceptable. The maximum deviation is less than .6%. We have also performed the reverse checking, i.e., using the measured velocity dispersion to calculate the dispersion of the attenuation based on the local approximation Eq. (6). We found that this relation is extremely sensitive to the curvature of the velocity dispersion. Higher order polynomial fitting of the velocity curve gives unreasonable results. Because the velocity dispersion is fairly small, we decided to use linear approximation to these velocity data, which created error less than the experimental uncertainty for the velocity fitting but gave good agreement to the measured attenuation dispersion. The results are shown in Figs.5 and 6 for the two different cut PZT samples.

Table II. The elastic, piezoelectric, dielectric constants and electromechanical coupling factors for poled piezoelectric ceramic PZT-5H measured by the different methods (the density $\rho = 7.36 \times 10^3 \text{ kg/m}^3$).

	M-1	M-2	M-3		M-1	M-2	M-3
Constant electric field				Elastic stiffness of			
Elastic stiffness	$(\times 10^{10} \text{N./m}^2)$			constant D	$(\times 10^{10} \text{N./m}^2)$		
c_{11}^E	11.3	11.3	11.5	c_{11}^D	11.5	11.5	11.7
c_{12}^E	6.73	6.73	6.85	c_{12}^D	6.91	6.88	7.02
c_{13}^E	6.69	6.58	6.89	c_{13}^D	5.87	5.81	6.09
c_{33}^E	9.89	9.79	10.15	c_{33}^D	13.6	13.6	14.1
c_{44}^E	2.01	2.01	2.03	c_{44}^D	3.59	3.59	3.60
c_{66}^E	2.30	2.30	2.33				
Elastic compliance				Elastic compliance			
of constant E	$(\times 10^{-12} \text{m}^2/\text{N})$			of constant D	$(\times 10^{-12} \text{m}^2/\text{N})$		
s_{11}^E	16.4	16.3	16.3	s_{11}^D	14.0	14.0	13.9
s_{12}^E	-5.32	-5.43	-5.23	s_{13}^D	-2.69	-2.69	-2.69
s_{13}^E	-7.52	-7.31	-7.51	s_{33}^D	10.8	10.7	10.7
s_{33}^E	20.3	20.5	20.0	s_{44}^D	27.8	27.8	27.8
s_{44}^E	49.8	49.8	49.3				
s_{66}^E	43.5	43.5	43.7				
Piezoelectric stress				Piezoelectric strain			
constant	(C/m^2)			constant	$(\times 10^{-12} \text{C/N})$		
e_{15}	14.8	14.8	14.7	d_{15}	735	735	726
e_{31}	-5.26	-4.85	-5.01	d_{31}	-263	-253	-262
e_{33}	23.5	23.8	24.0	d_{33}	515	512	518
Piezoelectric				Piezoelectric stiffness			
voltage constant	$(\times 10^{-3} \text{m}^2 \text{C}^{-1})$			constant	$(\times 10^8 \text{NC}^{-1})$		
g_{15}	29.9	29.9	29.5	h_{15}	10.7	10.7	10.6
g_{31}	-9.36	-9.02	-9.31	h_{31}	-3.52	-3.24	-3.35
g_{33}	18.4	18.3	18.4	h_{33}	15.7	15.9	16.0
Constant stress				Constant strain			
Dielectric constant				Dielectric constant			
ϵ_{11}^T	2778	2778	2778	ϵ_{11}^S	1550	1550	1567
ϵ_{33}^T	3170	3170	3170	ϵ_{33}^S	1691	1691	1691
Electromechanical							
Coupling factor							
k_{15}	0.664	0.664	0.660				
k_{31}	-0.387	-0.374	-0.386				
k_{33}	0.683	0.683	0.683				

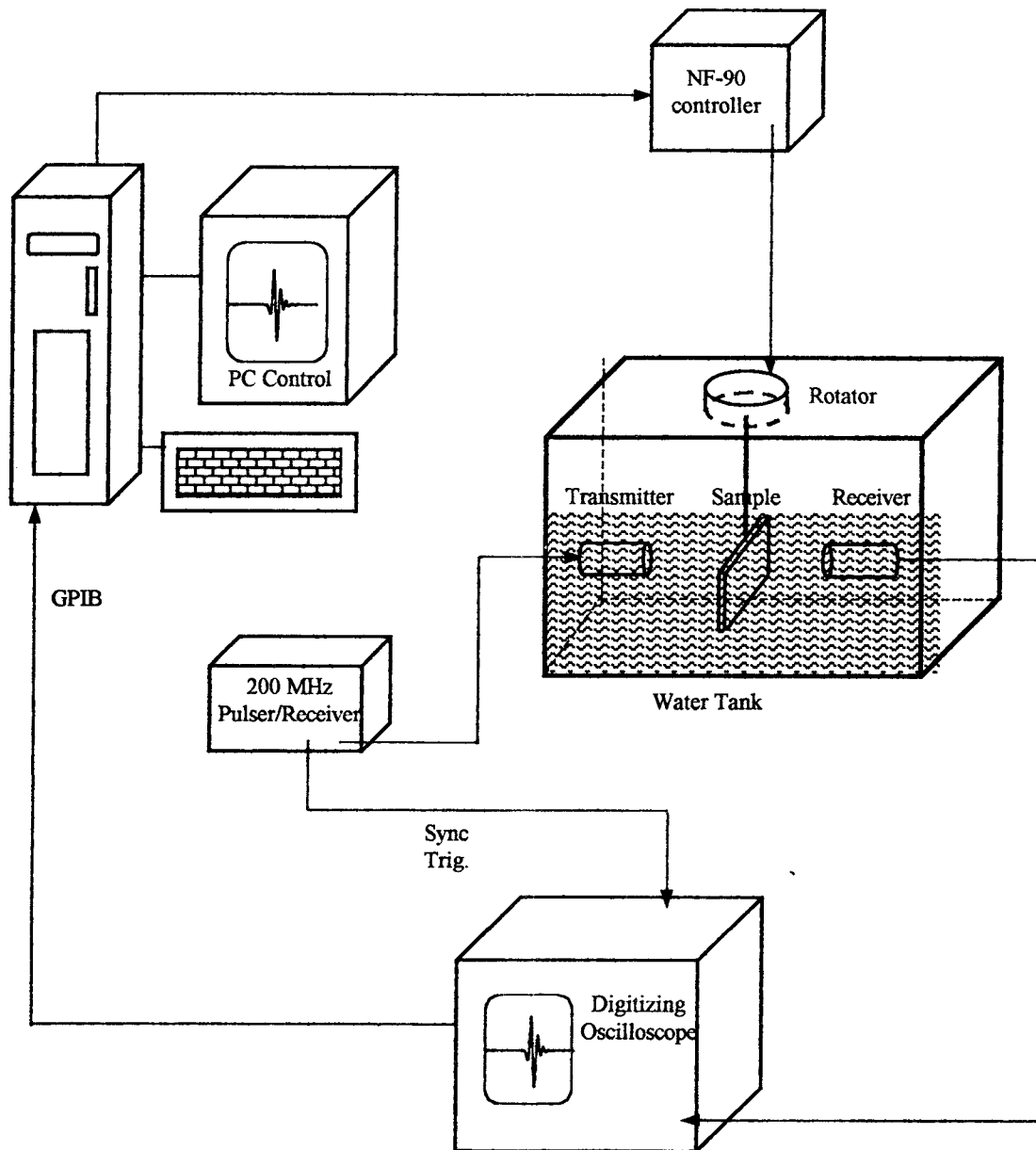
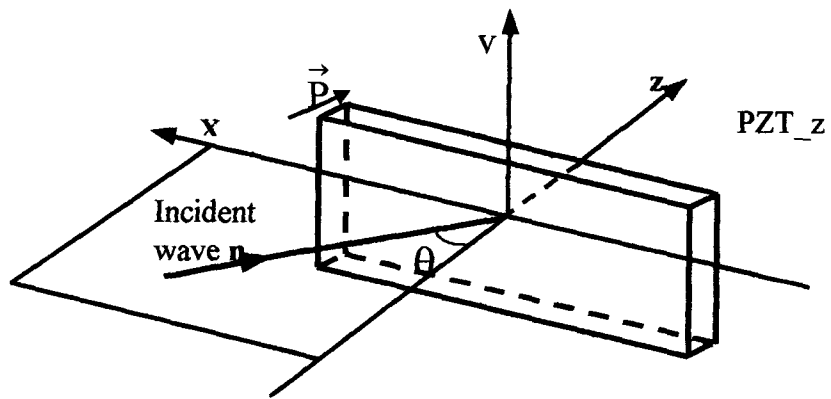
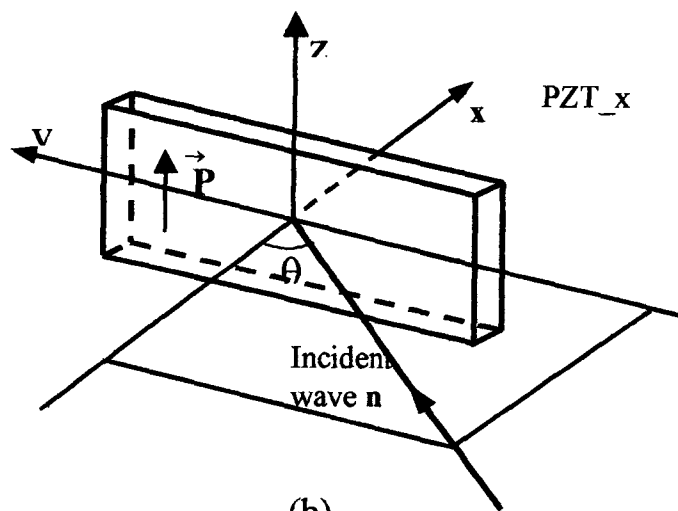


Fig. 1. Diagram of the ultrasonic experimental set up.



(a)



(b)

Fig. 2. (a) Incidence of a wave in the x-z plane of a PZT sample (PZT_z). (b) Incidence of a wave in the x-y plane of a PZT sample (PZT_x).

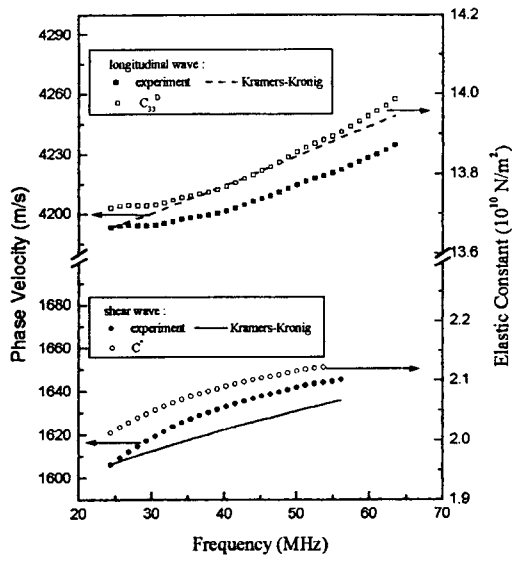


Fig. 3 Measured and calculated phase velocity and elastic constant dispersion for a wave propagating in the x-z plane of a PZT sample (PZT_z).

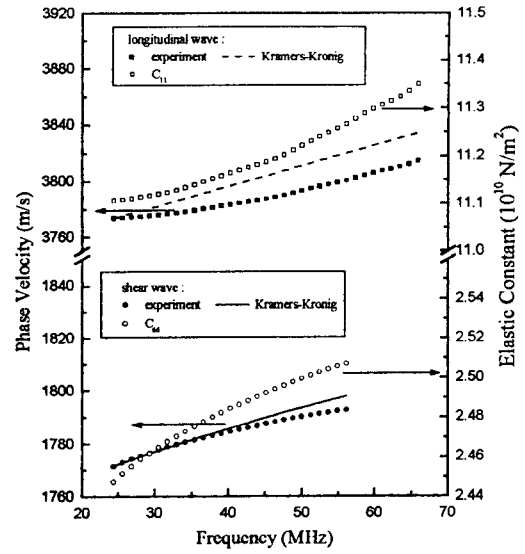


Fig. 4 Measured and calculated phase velocity and elastic constant dispersion for a wave propagating in the x-y plane of a PZT sample (PZT_x).

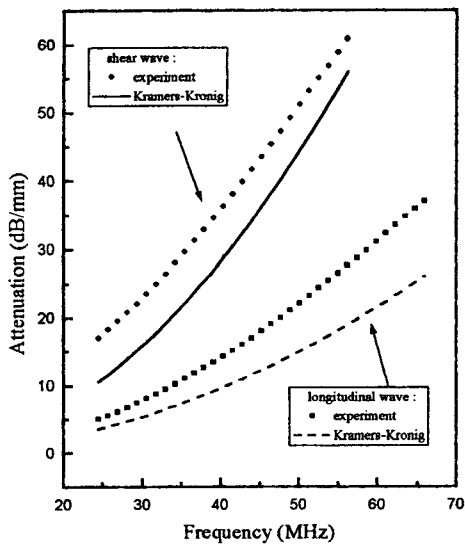


Fig. 5 Measured and calculated dispersion of ultrasonic attenuation for a wave propagating in the x-z plane of a PZT sample (PZT_z).

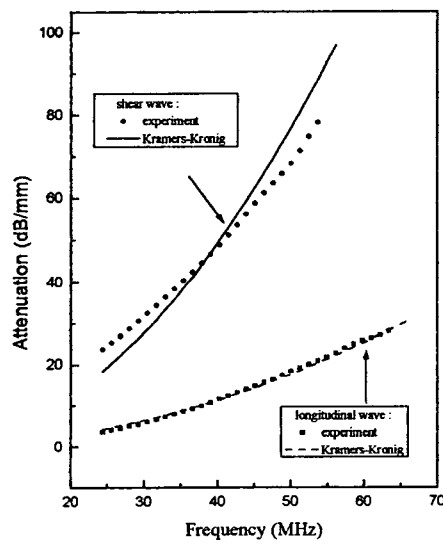


Fig. 6 Measured and calculated dispersion of ultrasonic attenuation for a wave propagating in the x-y plane of a PZT sample (PZT_x).

5. SUMMARY AND CONCLUSIONS

We have investigated thoroughly the characterization techniques to obtain reliable physical parameters of piezoelectric materials. A complete set of fundamental material constants for PZT-5H has been accurately determined by using ultrasonic technique assisted with resonance technique. The advantage of using the ultrasonic technique instead of the pure resonance technique is that the samples are required to have only one pair of precisely aligned faces and there is no aspect ratio requirement. Moreover, fewer samples are used when combine the two techniques, which increases self-consistency of the measured material parameters.

The dispersions of velocity and attenuation for piezoceramic PZT-5H were investigated by using ultrasonic spectroscopy at the frequency range of 20-65 MHz. In the investigated frequency range, velocity dispersion of 1-3m/s per MHz was observed. The attenuation depends nonlinearly on frequency and the shear wave exhibited an order of magnitude larger attenuation than the longitudinal wave. We also showed that the Kramers-Kronig relations between velocity dispersion and attenuation dispersion are satisfied for the longitudinal waves. However, for the shear waves, the agreement between experiments and theory was not as satisfactory, indicating the nonlinear origin of the shear wave attenuation.

6. REFERENCE

1. W. P. Mason, "Piezoelectric crystals and their application to ultrasonic", *D. Van Nostrand Co., Inc., New York*, 1950.
2. "IRE standards on piezoelectric crystals, 1949", *Proc. IRE*, **37**, pp.1378-1395, 1949.
3. "IRE standards on piezoelectric crystals – the piezoelectric vibrator: definitions and methods of measurement, 1957", *Proc. IRE*, **45**, pp. 353 – 358, 1957.
4. "IRE standards on piezoelectric crystals: determination of the elastic, piezoelectric, and dielectric constants–the electromechanical coupling factor, 1958", *Proc. IRE* **46**, pp.764-778, 1958.
5. "IEEE standard on piezoelectricity, ANSI/IEEE std, 176-1987", *IEEE, New York*, 1987.
6. W. Cao, S. N. Zhu and B. Jiang, "Analysis of shear modes in a piezoelectric vibrator", *J. Appl. Phys.* **83**, pp. 4415-4420, 1998.
7. J. J. Kyame, " Wave Propagation in Piezoelectric Crystals", *J. Acous. Soc. Amer.* **21**, pp. 159-167, 1949.
8. H. J. McSkimin, "Note and references for the measurement of elastic moduli by means of ultrasonic waves", *J. Acous. Soc.* **33**, pp. 606-616, 1961.
9. R. T. Smith and F. S. Welsh, Temperature dependence of the elastic, piezoelectric, and dielectric constants of lithium tantalate and lithium niobate", *J. Appl. Phys.* **42**, pp. 2219-2230, 1971.
10. D. Berlincourt and H. Jaffe, " Elastic and piezoelectric coefficients of single-crystal barium titanate", *Phys. Rev.* **111**, pp. 143-148, 1958.
11. Wenwu Cao and G. R. Barsch, "Elastic Constants of KMnF₃ as Functions of Temperature and Pressure" *Phys. Rev. B*, **38**, pp. 7947-7958 (1988).
12. H. F. Wang, W. Jiang and W. Cao, "Characterization of Lead Zirconate Titanate Piezoelectric Ceramic Using High frequency Spectroscopy", *J. Appl. Phys.* **85**, pp. 8083-8091, 1999.
13. M. O'Donnell, E. T. Jaynes and J. G. Miller, *J. Acoust. Soc. Am.*, **69**, 696-701, 1981.